



ELSEVIER

Available online at [www.sciencedirect.com](http://www.sciencedirect.com)

SCIENCE @ DIRECT®

Computer Vision  
and Image  
Understanding

Computer Vision and Image Understanding 94 (2004) 140–167

[www.elsevier.com/locate/cviu](http://www.elsevier.com/locate/cviu)

## Selection weighted vector directional filters

Rastislav Lukac,<sup>a,\*</sup> Bogdan Smolka,<sup>b</sup>  
Konstantinos N. Plataniotis,<sup>a</sup> and  
Anastasios N. Venetsanopoulos<sup>a</sup>

<sup>a</sup> *The Edward S. Rogers Sr. Department of ECE, University of Toronto,  
10 King's College Road, Toronto, M5S 3G4, Canada*

<sup>b</sup> *Department of Automatic Control, Silesian University of Technology,  
Akademicka 16 Str., 44-101 Gliwice, Poland*

Received 1 December 2002; accepted 29 October 2003

---

### Abstract

In this paper, a class of weighted vector directional filters (WVDFs) based on the selection of the output sample from the multichannel input set is analyzed and optimized. The WVDF output minimizes the sum of weighted angular distances to other input samples from the filtering window. Dependent on the weighting coefficients, the class of the WVDFs can be designed to perform a number of smoothing operations with different properties, which can be applied for specific filtering scenarios. In order to adapt the weighting coefficients to varying noise and image statistics, we introduce a methodology, which achieves an optimal trade-off between smoothing and detail preserving characteristics. The proposed angular optimization algorithms take advantage of adaptive stack filters design and weighted median filtering framework. The optimized WVDFs are able to remove image noise, while maintaining excellent signal-detail preservation capabilities and sufficient robustness for a variety of signal and noise statistics.

© 2003 Elsevier Inc. All rights reserved.

*Keywords:* Multichannel image processing; Impulsive noise; Directional processing of color images; Order-statistic theory; Weighted median filters; Optimization

---

\* Corresponding author. Fax: +1-416-978-4425.

E-mail address: [lukacr@ieee.org](mailto:lukacr@ieee.org) (R. Lukac).

## 1. Introduction

Images acquired by a sensor or transmitted through noisy information channel can often interfere with noise [2,6]. Noise introduced into the images may corrupt any of the following image processing steps mostly related [25] to image analysis (edge detection, image segmentation, and pattern recognition) and computer vision applications. Therefore, noise filtering [2,25,26,33], is one of the most important image processing steps usually viewed as the pre-processing methods. Its goal is the removal of unprofitable information in digital images without degradation of the underlying image structures. It is evident that noise filtering and image enhancement are an essential part of any image processing system [25] whether the final image is utilized for visual interpretation or for automatic analysis.

Multichannel signal processing [1,33,39] has been the subject of extensive research during the last years, primarily due to its importance to color image processing. Many of the techniques used for color noise reduction are direct modification (componentwise or marginal filters) [34,46] of the methods used for gray scale imaging [29]. Note that the independent processing of color image channels is inappropriate and leads to strong artifacts, especially when the filtering schemes [30] are based on the popular and robust order-statistic theory [2,31]. It has been widely recognized that the processing of color image data as vector fields is desirable due to the correlation that exists between the image channels and that the nonlinear vector processing of color images is the most effective way to filter out noise [27,33]. Therefore, the new filtering technique presented in this paper is also nonlinear and utilizes the correlation among the color image channels.

A number of nonlinear multichannel filters, which utilize correlation among multivariate vectors using various distance measures, have been proposed. The most popular multichannel filters are based on the ordering of vectors [1,24,30,38] in a predefined sliding window. The output of these filters is defined as the lowest ranked vector according to a specific ordering technique based on vectors' directions and vectors' magnitude. In general, vectors' magnitude constitutes a measure of their intensity (brightness), whereas the direction of vector samples describes their chromaticity [25].

Probably the most well-known filter is the vector median filter (VMF) [1]. The VMF can be derived as a maximum likelihood estimate (MLE), when the underlying probability densities of input samples are double exponential.

Vector directional filters (VDFs) [39] operate on the direction of the image vectors and such an approach is referred as directional processing. Applying this filtering technique, image vectors with atypical directions in the vector space are eliminated and vector directional filters result in optimal estimates in the sense of color chromaticity [27].

Research [39] described theory related to the analysis of statistical and deterministic properties of the basic vector directional filter (BVDF), which is a fundamental filtering scheme designed within the VDF framework. Note that the BVDF output direction is the MLE of directions of the input vectors [27]. Because of insufficient performance of the BVDF, work [39] also introduced its extensions such as the

generalized vector directional filters (GVDFs), spherical medians, double window GVDF followed by an  $\alpha$ -trimmed mean or by a multistage max-median filter. Another improvement was achieved by introducing vector median-vector directional hybrid filters (HVF) [12], fuzzy VDF [32] and directional distance filter (DDF) [18].

This paper focuses on a new class of weighted vector directional filters (WVDFs) as a natural extension of the BVDF. The proposed filters can offer better detail-preserving characteristics, higher flexibility of a filter design and less computational complexity in comparison with the extensions of the BVDF. In addition to these properties, the proposed method outperforms in terms of subjective and objective image quality measures the widely used standard vector approaches such as VMF, BVDF, and DDF. We also provide the optimization tool for adapting the WVDF non-negative real weights to signal and noise statistics by a new angular multichannel generalization of the adaptive least mean absolute (LMA) optimization routines used in the design of weighted median filters of gray-scale images. Using the proposed angular optimization scheme, it is possible to adapt the WVDF weighting coefficients under the constraint of negative weights to varying signal and noise statistics and achieve an excellent balance between the signal-detail preservation and the noise attenuation.

The rest of this paper is organized as follows. In the next Section, weighted median filters and their adaptive optimization algorithms are described. Section 3 focuses on the well-known VMF. Section 4 presents the VDF filtering class, which utilizes the directional ordering of input samples. In Section 5, we provide a new class of WVDFs and analyze them in terms of weighting vectors and the obtained smoothing concept. We also provide new approaches to the adaptation of WVDFs to varying signal and noise statistics, taking advantage of adaptive stack filter design and weighted median filter structure. Section 6 is devoted to the analysis of the proposed WVDF framework in its dependence on filter parameters and the intensity of impulsive noise corruption. This section contains a number of simulations, tests and filtering results, together with tables and graphs depicting the objective image quality measures. Finally, main ideas, results and future work are summarized in Section 7.

## 2. Weighted median filters

Weighted median (WM) filters [2,31] constitute an important nonlinear filtering class. Their robust smoothing capability in environments impulsive in nature and flexible design [28] in conjunction with an optimization framework [43,44] make this filtering class sufficiently attractive. Moreover, the WM filters are computationally efficient because their implementation takes advantage of binary operations [3,41] and analysis [23,45].

Let  $V(n) = \{x_1(n), x_2(n), \dots, x_N(n)\}$  be an input set of gray-scale image samples determined by a filter window of a finite odd length  $N$ , where  $n = 0, 1, \dots, Q - 1$  denotes the position of the filtering window centered in the  $x(n) = x_{(N+1)/2}(n)$  and  $Q$  is the signal length. Let each input sample  $x_i(n)$  be associated with a real valued

weight  $w_i$ , for  $i = 1, 2, \dots, N$ . The weighted median of the input set  $V(n)$  is the sample  $y(n) \in V(n)$  minimizing the following expression:

$$f(y(n)) = \sum_{i=1}^N w_i |y(n) - x_i(n)|. \quad (1)$$

If each weight  $w_i$  is equal to 1, the WM filter is equivalent to the well-known median filter (MF) [29,31]. In order to choose an appropriate weight vector, so that the WM filter would be able to remove impulses and simultaneously preserve all desired image features, some optimization algorithms [42,44], that originate from the stack filter design [7,43], have been developed. The adaptive algorithms described in this paper are based on linear and sigmoidal approximations of the sign function.

Given an input set  $V(n)$  and a weight vector  $\mathbf{w} = \{w_1, w_2, \dots, w_N\}$ , the WM output is denoted as  $y(n) = y(\mathbf{w}, V(n))$ . Estimating a desired signal  $o(n)$  is accompanied with the estimation error  $e(n) = o(n) - y(n)$ . Then, the cost function defined under the mean absolute error (MAE) and the mean square error (MSE) is defined as

$$J_{\text{MAE}}(\mathbf{w}, n) = E\{|o(n) - y(\mathbf{w}, V(n))|\}, \quad (2)$$

$$J_{\text{MSE}}(\mathbf{w}, n) = E\{(o(n) - y(\mathbf{w}, V(n)))^2\}, \quad (3)$$

where  $E\{\cdot\}$  represents statistical expectation used to guarantee the minimum average loss or risk. With the constraint of non-negative weights, the optimization problem with inequality constraints can be expressed as follows:

$$\text{minimize } J_{\text{MAE}}(\mathbf{w}, n) \text{ or } J_{\text{MSE}}(\mathbf{w}, n) \quad \text{subject to } w_i \geq 0, \text{ for } i = 1, 2, \dots, N. \quad (4)$$

Both cost functions (2) and (3) appear to be non-convex in the weights and are characterized by multiple local minimum. Under the assumption that the optimal weights are at one of the local minima, the conditions for optimality can be derived as follows:

$$\frac{\partial J_{\text{MAE}}(\mathbf{w}, n)}{\partial w_i} = \frac{\partial}{\partial w_i} E\{|o(n) - y(\mathbf{w}, V(n))|\}, \quad (5)$$

$$= E\left\{ \text{sgn}(o(n) - y(n)) \frac{\partial y(n)}{\partial w_i} \right\}, \quad (6)$$

and

$$\frac{\partial J_{\text{MSE}}(\mathbf{w}, n)}{\partial w_i} = 2E\left\{ (o(n) - y(n)) \frac{\partial y(n)}{\partial w_i} \right\}, \quad (7)$$

where

$$\text{sgn}(a) = \begin{cases} 1 & a > 0 \\ 0 & a = 0 \\ -1 & a < 0 \end{cases} \quad (8)$$

is the sign function.

Assuming the MAE criteria, the necessary condition for the filter optimality is given by

$$\left\{ \text{sgn}(o(n) - y(n)) \frac{\partial y(n)}{\partial w_i} \right\} = 0, \quad w_i \geq 0, \quad \text{for } i = 1, 2, \dots, N. \quad (9)$$

With respect to this analysis, adaptive WM algorithms were developed based on linear [43] and sigmoidal approximation [44] of the sign function. Using the least mean square (LMS)-type formulation and the constraint of non-negative weighting coefficients, the adaptation step related to (2) is given by

$$w_i(n+1) = P \left[ w_i(n) + 2\mu \frac{\partial J(\mathbf{w}, n)}{\partial w_i} \right], \quad (10)$$

where  $i = 1, 2, \dots, N$ , and  $P(\cdot)$  is a projection function

$$P(w_i(n)) \approx \begin{cases} 0 & \text{if } w_i(n) < 0 \\ w_i(n) & \text{otherwise} \end{cases} \quad (11)$$

which changes the negative values to zero.

Replacing the statistical expectation in (6) with the instantaneous estimates results in the following adaptation formula:

$$w_i(n+1) = P \left[ w_i(n) + 2\mu \frac{\partial y(\mathbf{w}, n)}{\partial w_i} \text{sgn}(o(n) - y(n)) \right], \quad (12)$$

where  $e(n) = o(n) - y(n)$  is the error at the  $n$ th iteration.

Applying the principle of minimum error criterion with the simultaneous principle of orthogonality, adaptation formula (12) is redefined as follows:

$$w_i(n+1) = P[w_i(n) + 2\mu(o(n) - y(n))(x_i(n) - o(n))]. \quad (13)$$

Let us consider the sliding filtering window related to the position  $n$ , moving over an image domain. During processing, the weight coefficients are adjusted by adding the contribution of the samples multiplied by a certain regulation factor. If the adaptive WM algorithm based on the sigmoidal approximation of the sign function is considered, an adjustment of the filter weights can be expressed [44] as follows:

$$w_i(n+1) = P[w_i(n) + 2\mu(o(n) - y(n))\text{sgn}_s(x_i(n) - y(n))], \quad (14)$$

where  $i = 1, 2, \dots, N$ ,  $P(\cdot)$  is a projection function (11),  $o(n)$  is the desired sample,  $y(n)$  is the WM output,  $\mu$  is the iteration constant and  $\text{sgn}_s(\cdot)$  is the sign function approximated by the sigmoidal function

$$\text{sgn}_s(a) = \frac{2}{1 + e^{-a}} - 1. \quad (15)$$

Let us consider that  $P(\cdot)$  is an identity function, whose argument remains unchanged. If  $x_i(n) \gg y(n)$  and  $\mu$  is positive, the adaptation formula (14) is given by

$$w_i(n+1) = w_i(n) + 2\mu(o(n) - y(n)), \quad (16)$$

i.e., the importance of the sample occupying the  $i$ th position in a supporting window increases if  $o(n)$  is greater than the actual WM output  $y(n)$  and decreases if  $o(n)$  is less than  $y(n)$ . Thus, this difference multiplied by regularization factor represents the weight increment (for  $0 < o(n) - y(n)$ ), the weight decrement (for  $0 > o(n) - y(n)$ ) or it can remain the weights unchanged (for  $o(n) - y(n) = 0$ ). In general, the initial weight vector  $\mathbf{w}(0)$  can be set to arbitrary positive values, but the best idea is to start the weight adaptation with equal weights corresponding to the median. Regarding the best value of  $\mu$ , research [44] showed that the algorithm converges to sub-optimal solution for sufficiently small positive value of  $\mu$ , e.g.,  $10^{-5}$ .

In the case of adaptive WM filtering with the linear approximation [43], the weight coefficients are updated as follows:

$$w_i(n+1) = P \left[ w_i(n) + 2\mu \left[ x_{\max}(n) - x_{\min}(n) - 2|o(n) - x_i(n)| - \sum_{j=1}^N w_j(n)(x_{\max}(n) - x_{\min}(n) - 2|x_i(n) - x_j(n)|) \right] \right], \quad (17)$$

where  $i = 1, 2, \dots, N$ ,  $j = 1, 2, \dots, N$ ,  $x_{\max}(n)$  and  $x_{\min}(n)$  represent the maximum and the minimum of the input set  $\{x_1(n), x_2(n), \dots, x_N(n)\}$ , respectively, and  $\mu$  is the positive adaptation stepsize [43]. Note that the WM optimization with the linear approximation of the sign function is also restricted by a projection operation  $P(\cdot)$  defined by (11).

### 3. Vector median filter

In the last decade, a variety of filtering methods for multichannel image processing were provided [1,33,39]. The common feature of vector filters lies in the consideration of the inherent correlation that exists between the image color channels. Since the vector approaches process an input signal as a set of vectors, color artifacts to which the human visual system is very sensitive [35] cannot be created as a filter output.

If the image information interferes with impulsive noise [2,6], filters based on the robust order-statistic theory provide an efficient solution. Note that the direct extension of the order-statistic theory to color images is impossible due to their vectorial nature [38]. Therefore, the observed samples are ordered according to specially developed distance functions.

Let  $y(x) : Z^l \rightarrow Z^m$  represent a multichannel image, where  $l$  is an image dimension and  $m$  denotes the number of color channels. In the case of standard color images, parameters  $l$  and  $m$  are equal to 2 and 3, respectively. Let  $W(n) = \{\mathbf{x}_i(n) \in Z^l; i = 1, 2, \dots, N\}$  represent a filter window of a finite size  $N$ , where  $\mathbf{x}_1(n), \mathbf{x}_2(n), \dots, \mathbf{x}_N(n)$  is a set of noisy samples and the central sample  $\mathbf{x}(n) = \mathbf{x}_{(N+1)/2}(n)$  determines the position of the filter window. Note that  $x_{ik}(n)$ , for  $k = 1, 2, \dots, m$ , is the  $k$ th element of the input sample  $\mathbf{x}_i(n) = (x_{i1}(n), x_{i2}(n), \dots, x_{im}(n))$ . Like in the previous Section,  $n = 0, 1, \dots, Q - 1$  characterizes the position of running window and  $Q$  is the signal length.

Let us consider that each input multichannel sample  $\mathbf{x}_i$  is associated with the distance measure

$$L_i(n) = \sum_{j=1}^N \|\mathbf{x}_i(n) - \mathbf{x}_j(n)\|_\gamma \quad \text{for } i = 1, 2, \dots, N, \quad (18)$$

where  $\|\mathbf{x}_i(n) - \mathbf{x}_j(n)\|_\gamma$  quantifies the distance between two  $m$ -channel samples  $\mathbf{x}_i(n)$  and  $\mathbf{x}_j(n)$  using the generalized Minkowski metric [9] given by

$$\|\mathbf{x}_i(n) - \mathbf{x}_j(n)\|_\gamma = \left( \sum_{k=1}^m |x_{ik}(n) - x_{jk}(n)|^\gamma \right)^{\frac{1}{\gamma}} \quad (19)$$

where  $x_{ik}(n)$  is the  $k$ th element of  $\mathbf{x}_i(n)$  and  $\gamma$  characterizes the used norm. The Minkowski metric includes [33] the city-block distance ( $\gamma = 1$ ), Euclidean distance ( $\gamma = 2$ ) and chess-board distance ( $\gamma = \infty$ ) as the special cases.

Let us assume that the ordering of the aggregated distances of (18) given by

$$L_{(1)}(n) \leq L_{(2)}(n) \leq \dots \leq L_{(N)}(n) \quad (20)$$

implies the the same ordering scheme to the input set  $W(n)$ . This procedure results in the ordered sequence

$$\mathbf{x}_{(1)}(n) \leq \mathbf{x}_{(2)}(n) \leq \dots \leq \mathbf{x}_{(N)}(n). \quad (21)$$

The sample  $\mathbf{x}_{(1)}(n) \in W(n)$  associated with the minimum aggregated distance  $L_{(1)}(n) \in \{L_1(n), L_2(n), \dots, L_N(n)\}$  constitutes the VMF output [1]. This lowest order-statistics minimizes the distance to other samples inside the sliding filtering window  $W(n)$ .

#### 4. Directional processing of color images

VDFs [39] employ a vector ordering technique in which the angle between image vectors serves as the ordering criterion. Since vectors such as multichannel samples are uniquely characterized by their direction and magnitude, these features can be exploited in the design of vector filtering classes. Note that the filtering schemes based on directional processing of color images (or directional processing followed by magnitude processing) may achieve better performance in comparison with the VMF based approaches.

##### 4.1. Vector directional filters

In the directional processing of color images [22,27,32,39], each input color vector  $\mathbf{x}_i(n)$  is associated with the aggregated angular measure

$$\alpha_i(n) = \sum_{j=1}^N A(\mathbf{x}_i(n), \mathbf{x}_j(n)) \quad \text{for } i = 1, 2, \dots, N, \quad (22)$$

where

$$A(\mathbf{x}_i(n), \mathbf{x}_j(n)) = \cos^{-1} \left( \frac{\mathbf{x}_i(n) \cdot \mathbf{x}_j(n)}{|\mathbf{x}_i(n)| |\mathbf{x}_j(n)|} \right), \quad (23)$$

$$= \cos^{-1} \left( \frac{x_{i1}(n)x_{j1}(n) + x_{i2}(n)x_{j2}(n) + \cdots + x_{im}(n)x_{jm}(n)}{\sqrt{x_{i1}^2(n) + x_{i2}^2(n) + \cdots + x_{im}^2(n)} \sqrt{x_{j1}^2(n) + x_{j2}^2(n) + \cdots + x_{jm}^2(n)}} \right) \quad (24)$$

represents the angle between two  $m$ -dimensional vectors  $\mathbf{x}_i(n)$  and  $\mathbf{x}_j(n)$ .

If angular distances (22) serve as an ordering criterion, i.e.,

$$\alpha_{(1)}(n) \leq \alpha_{(2)}(n) \leq \cdots \leq \alpha_{(r)}(n) \leq \cdots \leq \alpha_{(N)}(n), \quad (25)$$

and this implies the same ordering scheme for the input samples of  $W(n)$ , the procedure results in

$$\mathbf{x}_{(1)}(n) \leq \mathbf{x}_{(2)}(n) \leq \cdots \leq \mathbf{x}_{(r)}(n) \leq \cdots \leq \mathbf{x}_{(N)}(n). \quad (26)$$

The lowest order-statistics  $\mathbf{x}_{(1)}(n)$  associated with the minimum angular distance  $\alpha_{(1)}(n)$  represents the BVDF output [39]:

$$\mathbf{y}_{\text{BVDF}}(n) = \mathbf{x}_{(1)}(n). \quad (27)$$

Since the VDFs and passas to a filter output a sample from a sample set ordered according to the sum of vector angles, these filters preserve color chromaticity of the input vectors much better than the VMF technique.

The set of the first  $r$  terms of (26) with simultaneous consideration of (25) constitutes the GVDF filtering scheme defined by

$$\mathbf{y}_{\text{GVDF}}(n) = \{\mathbf{x}_{(1)}(n), \mathbf{x}_{(2)}(n), \dots, \mathbf{x}_{(r)}(n)\} \quad (28)$$

The GVDF passes to the filter output the set of  $r$  vectors whose angle  $\alpha_i(n)$ , for  $i = 1, 2, \dots, N$ , to all other vectors inside the filter window  $W(n)$  is relatively small. Simply, the GVDF produces a set of vectors with similar directions in color space, and therefore the samples with atypical directions are eliminated. To choose one output sample, the GVDF filter is accompanied with an additional filter [33,39], processing the samples  $\mathbf{x}_{(1)}(n), \mathbf{x}_{(2)}(n), \dots, \mathbf{x}_{(r)}(n)$  according to their magnitude. Usually, the output set of the GVDF technique serves in the second level of processing as an input for an additional filter, e.g.,  $\alpha$ -trimmed average filter, multistage median filter and morphological filters. These filters process the samples  $\mathbf{x}_{(1)}(n), \mathbf{x}_{(2)}(n), \dots, \mathbf{x}_{(r)}(n)$  according to their magnitude, since these vectors have approximately equal directions in a vector space. Thus, the GVDF splits the color image processing into directional and magnitude processing. The drawback of such an approach is that it heavily increases the computational complexity of the VDFs.

#### 4.2. Hybrid filtering schemes

Developed later, the DFF [18] and the HVFs [12] techniques combine both ordering criteria (18) and (22). This causes both approaches to be computationally demanding.

Consider the DDF scheme utilizing the power parameter  $p$  ranged from 0 to 1. This filters make use of hybrid ordering criteria expressed through a product of the aggregated Minkowski metrics (18) and the aggregated angular measure (22):

$$\Omega_i(n) = (L_i(n))^{1-p} \cdot (\alpha_i(n))^p \quad \text{for } i = 1, 2, \dots, N, \quad (29)$$

$$\Omega_i(n) = \left( \sum_{j=1}^N \|\mathbf{x}_i(n) - \mathbf{x}_j(n)\|_y \right)^{1-p} \cdot \left( \sum_{j=1}^N A(\mathbf{x}_i(n), \mathbf{x}_j(n)) \right)^p$$

for  $i = 1, 2, \dots, N$ . (30)

The DDF output is the sample  $\mathbf{x}_{(1)} \in \{W(n)\}$  minimizing (30), i.e., the sample associated with the smallest value  $\Omega_{(1)}(n)$  so that  $\Omega_{(1)}(n) \leq \Omega_{(2)}(n) \leq \dots \leq \Omega_{(N)}(n)$  for  $\Omega_{(i)} \in \{\Omega_1(n), \Omega_2(n), \dots, \Omega_N(n)\}$ . If  $p = 0$ , the DDF operates as the VMF, whereas for  $p = 1$ , the DDF is equivalent to the BVDF.

The introduction of the DDF inspired a new set of heuristic vector processing filters such as the HVFs [12], which try to capitalize on the same appealing principle, namely the simultaneous minimization of the distance functions used in the VMF and the BVDF. The HVFs operate on the direction and the magnitude of the color vectors independently and then combine them to produce a unique final output. The  $HVF_1$  technique, viewed as a nonlinear combination of the VMF and BVDF filters, produces an output according to the following rule:

$$\mathbf{y}_{HVF_1}(n) = \begin{cases} \mathbf{y}_{VMF}(n) & \text{if } \mathbf{y}_{VMF}(n) = \mathbf{y}_{BVDF}(n), \\ \left( \frac{|\mathbf{y}_{VMF}(n)|}{|\mathbf{y}_{BVDF}(n)|} \right) \mathbf{y}_{BVDF}(n) & \text{otherwise,} \end{cases} \quad (31)$$

where  $\mathbf{y}_{VMF}(n)$  is the VMF output,  $\mathbf{y}_{BVDF}(n)$  characterizes the BVDF output and  $|\cdot|$  denotes the magnitude of the vector.

Another more complex hybrid filter, which involves the utilization of an arithmetic mean filter (AMF), has also been proposed. The structure of this so-called adaptive hybrid filter ( $HVF_2$ ) is as follows:

$$\mathbf{y}_{HVF_2}(n) = \begin{cases} \mathbf{y}_{VMF}(n) & \text{if } \mathbf{y}_{VMF}(n) = \mathbf{y}_{BVDF}(n), \\ \mathbf{y}_{out1}(n) & \text{if } \sum_{i=1}^N |\mathbf{x}_i(n) - \mathbf{y}_{out1}(n)| < \sum_{i=1}^N |\mathbf{x}_i(n) - \mathbf{y}_{out2}(n)|, \\ \mathbf{y}_{out2}(n) & \text{otherwise,} \end{cases} \quad (32)$$

$$\mathbf{y}_{out1}(n) = \left( \frac{|\mathbf{y}_{VMF}(n)|}{|\mathbf{y}_{BVDF}(n)|} \right) \mathbf{y}_{BVDF}(n), \quad (33)$$

$$\mathbf{y}_{out2}(n) = \left( \frac{|\mathbf{y}_{AMF}(n)|}{|\mathbf{y}_{BVDF}(n)|} \right) \mathbf{y}_{BVDF}(n) \quad (34)$$

where  $\mathbf{y}_{AMF}(n)$  denotes the output of the arithmetic mean filter operating inside the same processing window positioned in  $n$ . Both hybrid filters defined in (31) and (32) are computationally demanding, since they require evaluation of both the VMF and

BVDF outputs. Thus, the two independent ordering schemes are applied to the input samples to produce a unique final output.

## 5. Proposed method

Low-pass vector filters, e.g., VMF and VDF, are used to remove impulses or outliers, i.e., high frequency elements in the image. The problem is that these multichannel schemes operating on a fixed supporting window introduce excessive smoothing, blur details and eliminate fine image structures [24,33]. To avoid these drawbacks the noise reduction filters should be designed so that noise-free samples remain unchanged during the filtering operation. In the last decade, a number of approaches were developed that expanded the possibilities of multichannel filter design. The most favored approaches relate to the adaptive filters [4,22] based on the switching between the smoothing function and no filtering, incorporate the structural information into the filter design [7,14,15,42] and increase the degree of freedom in the filter design by introducing the coefficients into the filter structure [11,40,44].

In multichannel filtering, state-of-the-art weighted multichannel filters take advantage of the WM filtering framework as well as the myriad filtering [16,17] of gray-scale images. Weighted vector median filters [40] have been introduced as the nearest multichannel extension of the WM framework with aspects of their optimization discussed in [21]. Another works dealt with structural contents of the images, especially with digital paths defined on the image domain [36,37]. In directional processing of color images, the weighted filtering schemes along with the optimization framework based on fuzzy sets have been introduced in [32,33] and this concept is understood as the normalized weighted sum of the input sample multiplied by filter weights.

In this paper, we provide selection weighted vector directional filters (WVDFs) that enhance the flexibility of the VDF schemes by a simple introduction of a non-negative weight vector into the filter structure. The proposed framework is the nearest extension of the VDFs and passes to a filter output the input sample minimizing the aggregated weighted angular distances to other samples inside the filtering window  $W(n)$ . Therefore, the proposed WVDF framework is capable of removing bit errors and outliers from the color image while preserving the desired structure and color information. Such applications [25] include television and video [19,34] as well as new emerging fields such as DNA microarrays [8,10], digital art reconstruction [5,20], automatic systems of visual inspection [13]. To adapt a filter behavior to varying image and noise statistics we provide a new optimization framework which can be viewed as the angular multichannel generalization of the WM optimization. The problems that hindered the introduction of such an optimization in the past relate to polarity (sign) in adaptation formulas (14) and (17).

### 5.1. Selection weighted vector directional filters

Let  $W(n) = \mathbf{x}_1(n), \mathbf{x}_2(n), \dots, \mathbf{x}_N(n)$  be a set of multichannel vector-valued samples spawned by a filter window of a finite size  $N$  and let  $\mathbf{x}_{(N+1)/2}(n)$  be a central sample

corresponding to the window reference position. Let us assume that  $w_1, w_2, \dots, w_N$  represent a set of positive real weights, where each weight  $w_j$ , for  $j = 1, 2, \dots, N$ , is associated with the input sample  $\mathbf{x}_j(n)$ . Then, the aggregated angular distance  $\beta_i(n)$  equivalent to the sum of weighted angular distances associated with the input sample  $\mathbf{x}_i(n)$  is given by

$$\beta_i(n) = \sum_{j=1}^N w_j A(\mathbf{x}_i(n), \mathbf{x}_j(n)) \quad \text{for } i = 1, 2, \dots, N, \quad (35)$$

where  $A(\mathbf{x}_i(n), \mathbf{x}_j(n))$  represents the angle (23) between two multichannel samples  $\mathbf{x}_i(n)$  and  $\mathbf{x}_j(n)$ .

Assuming that the ordering scheme given by ordered angular measures

$$\beta_{(1)}(n) \leq \beta_{(2)}(n) \leq \dots \leq \beta_{(N)}(n) \quad (36)$$

implies the same ordering scheme to input vector-valued samples inside  $W(n)$ , the procedure results in the ordered input set  $\mathbf{x}_{(1)}(n); \mathbf{x}_{(2)}(n); \dots; \mathbf{x}_{(N)}(n)$ .

The output of the WVDF is the sample  $\mathbf{x}_{(1)}(n) \in \{W(n)\}$  associated with the minimum weighted angular distance  $\beta_{(1)}(n) \in \{\beta_1(n), \beta_2(n), \dots, \beta_N(n)\}$ . Thus, the WVDFs are outputting the sample from the input set, so that the local distortion is minimized and no new color artifacts are produced.

WVDF filters constitute a generalized vector filtering class operating on the directional domain of color images. If all weight coefficients are set to the same value, all angular distances will have the same importance and the WVDF operation will be equivalent to the BVDF. If only the center weight can vary in the value, whereas other weights remain unchanged, i.e.,

$$w_i = \begin{cases} N - 2k + 2 & \text{for } i = (N + 1)/2, \\ 1 & \text{otherwise,} \end{cases} \quad (37)$$

where  $k = 1, 2, \dots, (N + 1)/2$  is a smoothing parameter, the WVDFs perform the center weighted vector directional filtering (CWVDF). In the case of the smoothing parameter  $k = 1$ , the central weight  $w_{(N+1)/2}$  has the maximum possible value  $w_{(N+1)/2} = N$  and the CWVDF performs the identity operation. This causes that the CWVDF output is equivalent to the unchanged input central sample  $\mathbf{x}_{(N+1)/2}$ . The larger value of  $k$  increases the smoothing capability of the CWVDF. For the maximum value of  $k$ , i.e.,  $k = (N + 1)/2$ , the CWVDF provides the maximum amount of smoothing, which is equivalent to the BVDF operation.

Let us consider that  $\mathbf{x}_{(1)}(n), \mathbf{x}_{(2)}(n), \dots, \mathbf{x}_{(N)}(n)$  is the set of multichannel order statistics achieved using the conventional angular ordering criteria (22). The sample  $\mathbf{x}_{(1)}(n)$  is the lowest ranked vector and  $\mathbf{x}_{(N)}(n)$  is the uppermost ranked sample. The WVDF output  $\mathbf{y}(\mathbf{w}, W(n))$  is a function of the weight vector  $\mathbf{w} = \{w_1, w_2, \dots, w_N\}$  and it can be expressed as the sample  $\mathbf{y}(n)$  minimizing

$$\mathbf{y}(\mathbf{w}, W) = \arg \min_{\mathbf{y}(n)} \sum_{i=1}^N w_i A(\mathbf{y}(n), \mathbf{x}_i(n)) = \arg \min_{\mathbf{y}(n)} F(\mathbf{y}(n)) \quad (38)$$

Then, the following statements can be declared:

1. The WVDF filter has only  $N$  independent parameters, since its output  $\mathbf{y}(\mathbf{w}, W(n))$  depends only on the weight vector  $\mathbf{w}$ .
2. The WVDF output corresponds to one of the local minimums of  $F(\mathbf{y}(n))$ .
3. The WVDF output  $\mathbf{y}(\mathbf{w}, W(n))$  is always within the range of the order-statistics  $\mathbf{x}_{(1)}(n)$  and  $\mathbf{x}_{(N)}(n)$ , corresponding to the minimum  $\alpha_{(1)}(n)$  and minimum  $\alpha_{(N)}(n)$  aggregated angular distances (22).
4. The WVDF output is restricted to the dynamic range of the input samples. Therefore, it cannot cause any new outliers and color artifacts.

### 5.2. Proposed angular optimization

The variety of smoothing operations provided by the WVDFs represents sufficient motivation for the optimization of their weighting coefficients. In general, filter optimization belongs to the most important tasks related to the filter design. The relationship between the pixel under consideration (window center) and each pixel in the filter window should be reflected in the decision for the weight coefficients. In the adaptive design, the weights provide the degree to which the input vector contributes to the output of the filter.

In this paper, we adaptively determine the sub-optimal WVDF weight vector. Using directional generalizations of sigmoidal and linear WM optimization approaches, the proposed methods is capable of tracking varying noise and image statistics.

Main problems related to the extension of the scalar expression (14) to the multichannel case is the modification of the sign function. The reason is the difficulty of determining the polarity of the distance measure between two multichannel samples. In order to solve this problem using the directional processing base calculation, we replace the difference between two scalar samples  $a$  and  $b$  with the angle between two multichannel samples  $\mathbf{a}$  and  $\mathbf{b}$ . The polarity of this distance measure is given by the difference between magnitudes of vectors  $\mathbf{a}$  and  $\mathbf{b}$ .

Let us consider the following transformation of the difference  $a - b$  between two scalar samples  $a$  and  $b$  leading to the generalized difference between two multichannel samples  $\mathbf{a}$  and  $\mathbf{b}$ :

$$D(\mathbf{a} - \mathbf{b}) = S(\mathbf{a}, \mathbf{b})A(\mathbf{a}, \mathbf{b}), \quad (39)$$

where

$$S(\mathbf{a}, \mathbf{b}) \approx \begin{cases} +1 & \text{for } |\mathbf{a}| - |\mathbf{b}| \geq 0, \\ -1 & \text{for } |\mathbf{a}| - |\mathbf{b}| < 0 \end{cases} \quad (40)$$

is the polarity function.

Note that the polarity function introduced here saves the sign of the difference between the scalar image samples  $a$  and  $b$ , since for a scalar case  $m = 1$  the magnitude of  $\mathbf{a}$  and  $\mathbf{b}$  is equivalent to  $a$  and  $b$ , respectively. The polarity function based (39) is used to design the angular WVDF adaptation mechanisms.

Given an input set  $W(n) = \mathbf{x}_{(1)}(n), \mathbf{x}_{(2)}(n), \dots, \mathbf{x}_{(N)}(n)$  and a weight vector  $\mathbf{w} = w_1, w_2, \dots, w_N$ , denote the WVDF output as  $\mathbf{y}(n) = \mathbf{y}(\mathbf{w}, W(n))$ . Following pure

directional processing, the processing error in filtering a desired signal  $\mathbf{o}(n)$  is defined as  $e(n) = A(\mathbf{o}(n), \mathbf{y}(n))$ , where  $A(\cdot)$  is the angle of two multichannel samples (23). Using a simple replacement of the scalar distance in the WM framework with the angle of multichannel samples (23), it is possible to avoid the complicated derivations and determine the cost functions corresponding to (2) and (3) as follows:

$$J_{\text{MAE}}(\mathbf{w}, n) = E\{A(\mathbf{o}(n)), \mathbf{y}(\mathbf{w}, W(n))\}, \quad (41)$$

$$J_{\text{MSE}}(\mathbf{w}, n) = E\{A^2(\mathbf{o}(n)), \mathbf{y}(\mathbf{w}, W(n))\}, \quad (42)$$

where  $E\{\cdot\}$  represents statistical expectation. With the constraint of non-negative weights, the optimization problem with inequality constraints is the same as (4) under (41) and (42).

Like in the WM design, both cost functions (41) and (42) appear to be non-convex in the weights and dispose with multiple local minimum. Assuming that the optimal weights are at one of the local minimums, the conditions for optimality are given by

$$\frac{\partial J_{\text{MAE}}(\mathbf{w}, n)}{\partial w_i} = E\left\{\text{sgn}(D(\mathbf{o}(n) - \mathbf{y}(n))) \frac{\partial \mathbf{y}(n)}{\partial w_i}\right\}, \quad (43)$$

$$\frac{\partial J_{\text{MSE}}(\mathbf{w}, n)}{\partial w_i} = 2E\left\{A(\mathbf{o}(n), \mathbf{y}(n)) \frac{\partial \mathbf{y}(n)}{\partial w_i}\right\}. \quad (44)$$

### 5.2.1. Angular sigmoidal approach

Let  $\{\mathbf{x}_1(n), \mathbf{x}_2(n), \dots, \mathbf{x}_N(n)\}$  be the input set of  $m$ -channel samples and  $\mathbf{o}(n)$  the desired (original or noise-free) sample. Let us consider that each input sample  $\mathbf{x}_i(n)$  be associated with the nonnegative real weight  $w_i(n)$ , for  $i = 1, 2, \dots, N$ . Then, we can modify the sigmoidal optimization (14) and formulate its directional generalization for the multichannel case as follows:

$$w_i(n+1) = P[w_i(n) + 2\mu D(\mathbf{o}(n) - \mathbf{y}(n)) \text{sgn}_s(D(\mathbf{x}_i(n) - \mathbf{y}(n)))], \quad (45)$$

where  $\mathbf{y}(n)$  is the the output of the sigmoidally optimized WVDF (SWVDF) scheme related to the actual weight coefficients  $w_1(n), w_2(n), \dots, w_N(n)$  and the spatial indicator  $n = 0, 1, \dots, Q - 1$ . Notation  $\mathbf{x}_i(n)$  describes the input sample with the  $i$ th position in the filter window  $W(n)$ . Function  $D(\cdot)$  denotes the transformation introduced in (39),  $\text{sgn}_s$  characterizes the sigmoidal function (15) and  $P(\cdot)$  is a projection function (11).

### 5.2.2. Angular linear approach

Let us now consider the generalized linear approximation of the sign function. The extension of the LMA algorithm (17) based on linear approximation of the sign function from the scalar case to the vector expression requires to determine the maximum and the minimum of the vector-valued input set  $W(n)$  and replace the absolute difference between two scalar samples with the angle (23) between the two multichannel samples. Let the uppermost ranked sample  $\mathbf{x}_{(N)}(n)$  associated with the maximum conventional angular distance measure (22) represent the maximum sample of the vector-valued input set  $W(n)$  and the lowest ranked vector  $\mathbf{x}_{(1)}(n)$  minimizing the

sum of angles to other input samples represent the minimum input sample of  $W(n)$ . Thus, the update of the weight coefficients in the adaptive WVDF scheme based on the linear approximation of the sign function (so-called LWVDF scheme) can be stated as follows:

$$w_i(n+1) = P[w_i(n) + 2\mu[D(\mathbf{x}_{(N)}(n) - \mathbf{x}_{(1)}(n)) - 2A(\mathbf{o}(n), \mathbf{x}_i(n))] - \sum_{j=1}^N w_j(n)[D(\mathbf{x}_{(N)}(n) - \mathbf{x}_{(1)}(n)) - 2A(\mathbf{x}_i(n), \mathbf{x}_j(n))]], \quad (46)$$

where  $i = 1, 2, \dots, N$ ,  $j = 1, 2, \dots, N$ , and  $\mu$  is the positive adaptation stepsize. The negative weight coefficients are modified by projection operation (11).

The restrictions of both adaptation algorithms (45) and (46) follows the WM optimization framework. The adaptation stepsize  $\mu$  should be set a certain small value (a sensitivity analysis is presented in next Section) and the obtained weight coefficients cannot be negative. Therefore, the negative weights are projected (42) to zero. The starting weight vector  $\mathbf{w}(0)$  may be set to arbitrary positive values, however, all weights in starting vector should have an equivalent importance. Moreover, the proposed optimization schemes require a learning signal like in the WM optimization.

## 6. Experimental results

The primary purpose of all filtering schemes presented in this paper is to remove impulses and outliers from the image. Therefore, original test images Lena (Fig. 1A)



Fig. 1. Test color images, (original and contaminated): (A) original image Lena, (B) 2% impulsive noise, (C) 5% impulsive noise, (D) 10% impulsive noise, (E) 15% impulsive noise, and (F) 20% impulsive noise.

and Peppers (Fig. 2A) have been corrupted by the impulsive noise [22,33], modeled as follows:

$$\mathbf{x}(n) = \begin{cases} \mathbf{v}(n) & \text{with probability } p_v, \\ \mathbf{o}(n) & \text{with probability } 1 - p_v, \end{cases} \quad (47)$$

where  $n$ , for  $n = 0, 1, \dots, Q - 1$ , characterizes the spatial position of the samples,  $Q$  is the signal length,  $\mathbf{o}(n)$  is the original sample,  $\mathbf{x}(n)$  represents the sample from the noisy image and  $p_v$  is the corruption probability (also referred to a percentage number of corrupted pixels). Noise vector  $\mathbf{v}(n) = (v_R(n), v_G(n), v_B(n))$  is independent from pixel to pixel and has generally much larger and smaller amplitude than the neighboring samples at least in one of the components.

The results were evaluated by the commonly used objective measures [2,33], such as MAE, MSE, and NCD. In designing the proposed method we will minimize these criteria and try to achieve the best balance between noise attenuation and preservation of the color/structural information.

Mathematically, the MAE and the MSE are given by

$$\text{MAE} = \frac{1}{mQ} \sum_{k=1}^m \sum_{n=0}^{Q-1} |o_k(n) - x_k(n)|, \quad (48)$$

$$\text{MSE} = \frac{1}{mQ} \sum_{k=1}^m \sum_{n=0}^{Q-1} (o_k(n) - x_k(n))^2, \quad (49)$$

where  $o_k(n)$  and  $x_k(n)$  denote the original and filtered (noisy) value, respectively, corresponding to the  $k$ th image channel and the  $n$ -th spatial position in a  $K_1 \times K_2$  color image. Note that  $n = 0, 1, \dots, Q - 1$ , for  $Q = K_1 K_2$ .

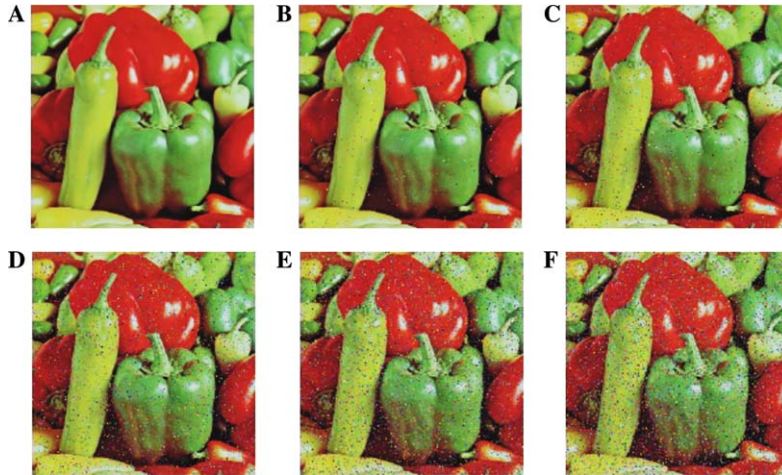


Fig. 2. Test color images, (original and contaminated): (A) original image Peppers, (B) 2% impulsive noise, (C) 5% impulsive noise, (D) 10% impulsive noise, (E) 15% impulsive noise, and (F) 20% impulsive noise.

The NCD criteria [33] expresses well the measure of the color distortion. The NCD is defined on the  $Lu^*v^*$  color space by

$$\text{NCD} = \frac{\sum_{n=0}^{Q-1} \sqrt{(L^o(n) - L^x(n))^2 + (u^o(n) - u^x(n))^2 + (v^o(n) - v^x(n))^2}}{\sum_{n=0}^{Q-1} \sqrt{(L^o(n))^2 + (u^o(n))^2 + (v^o(n))^2}}, \quad (50)$$

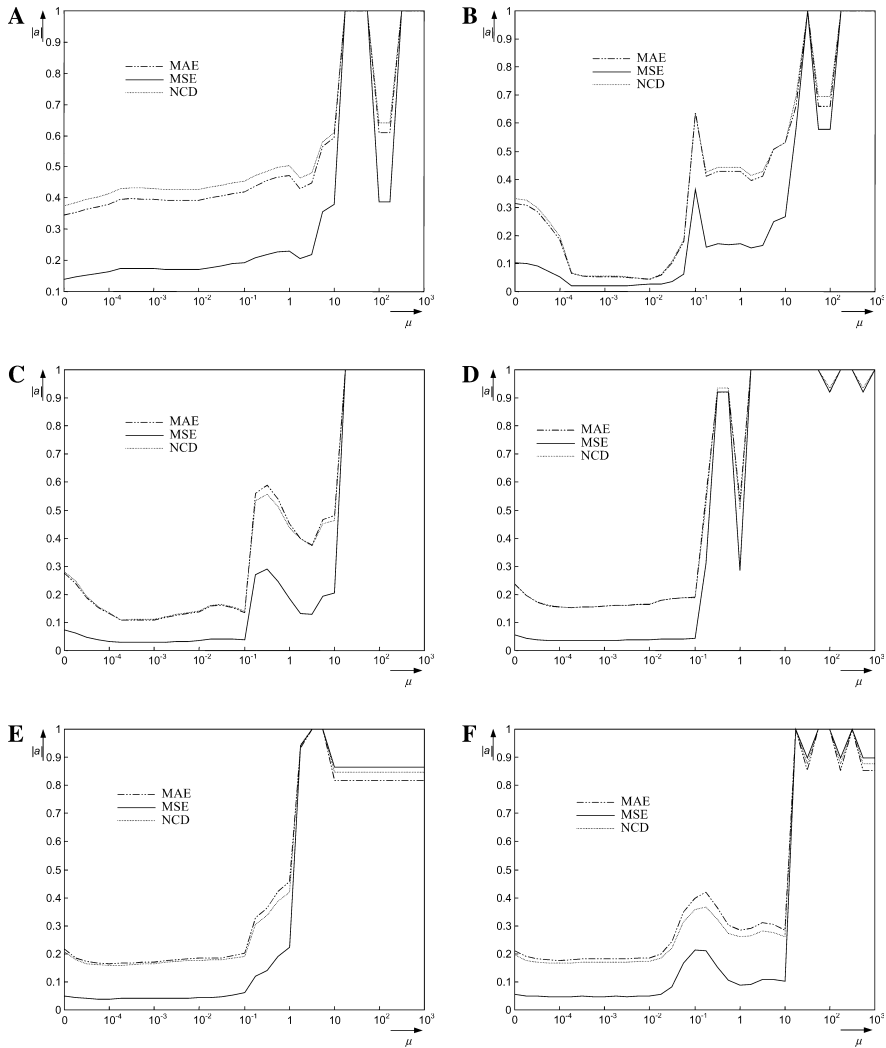


Fig. 3. WVDF linear optimization (LWVDF filter) expressed through objective quality measures dependent on the iteration stepsize  $\mu$ . Training set was obtained through the image Lena with: (A) no corruption, (B) 2% impulsive noise, (C) 5% impulsive noise, (D) 10% impulsive noise, (E) 15% impulsive noise, and (F) 20% impulsive noise.

where  $L^o(n), u^o(n), v^o(n)$  and  $L^x(n), u^x(n), v^x(n)$  are values of the lightness  $L$  and chromaticity components  $u, v$  of the original image sample  $\mathbf{o}(n)$  and the noisy image sample  $\mathbf{x}(n)$ , respectively.

The WVDF weighting coefficients were adapted for the color image filtering task using the well-known color test images Lena (Fig. 1A) and Peppers (Fig. 2A) and also their corrupted versions (Figs. 1B–F and Figs. 2B–F) contaminated with 2, 5, 10, 15, and 20% impulsive noise as the training sets, respectively. All filtering results were obtained with a  $3 \times 3$  square window and the number of samples  $N = 9$ .

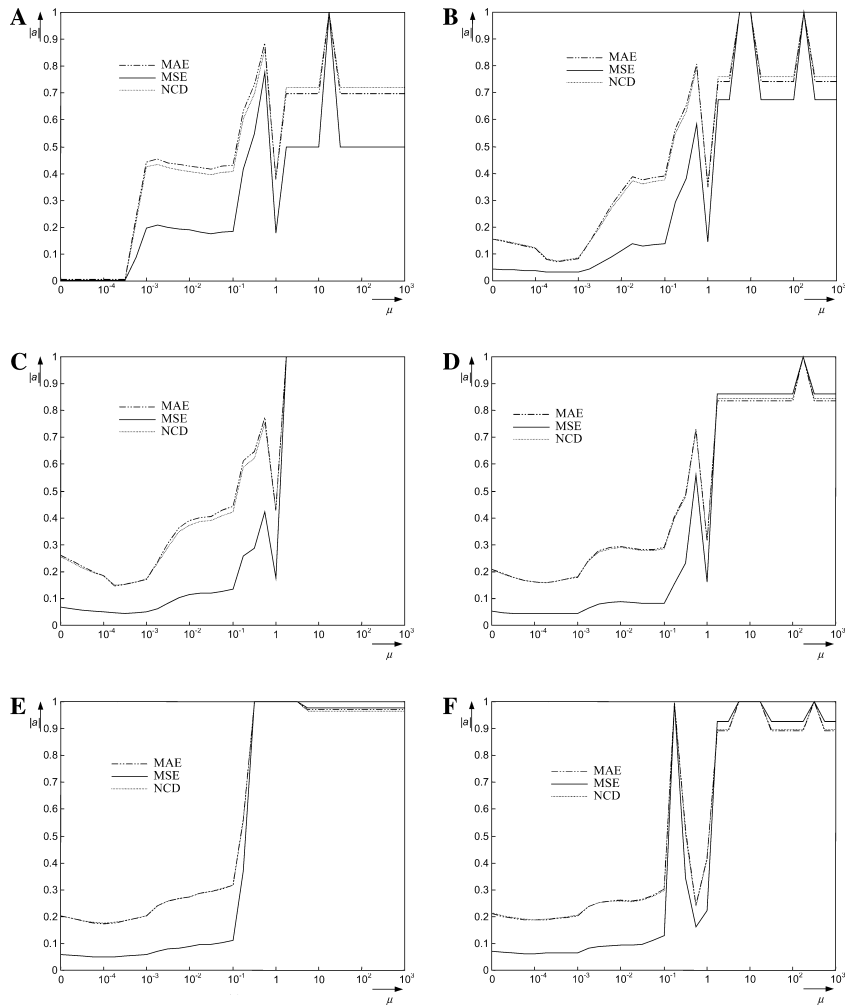


Fig. 4. WVDF linear optimization (LWVDF filter) expressed through normalized measures dependent on the iteration step size  $\mu$ . Training set was given by the image Peppers with: (A) no corruption, (B) 2% impulsive noise, (C) 5% impulsive noise, (D) 10% impulsive noise, (E) 15% impulsive noise, and (F) 20% impulsive noise.

The proposed WVDF optimization started with the same initial weighting vector  $\mathbf{w}(0) = [1, 1, 1, 1, 1, 1, 1, 1, 1]$  which corresponds to the BVDF operation. The achieved results are shown in Figs. 3–6 as functions of the image restoration quality measures in dependence on the value of the iteration constant  $\mu$ , which ranged from  $10^{-5}$  to  $10^3$ . The obtained results indicate that the performance of the WVDF based on linear approximation of the sign function (LWVDF), decreases with the increasing value of  $\mu$ . The most appropriate value of  $\mu$  related to the LWVDF (Fig. 3 and

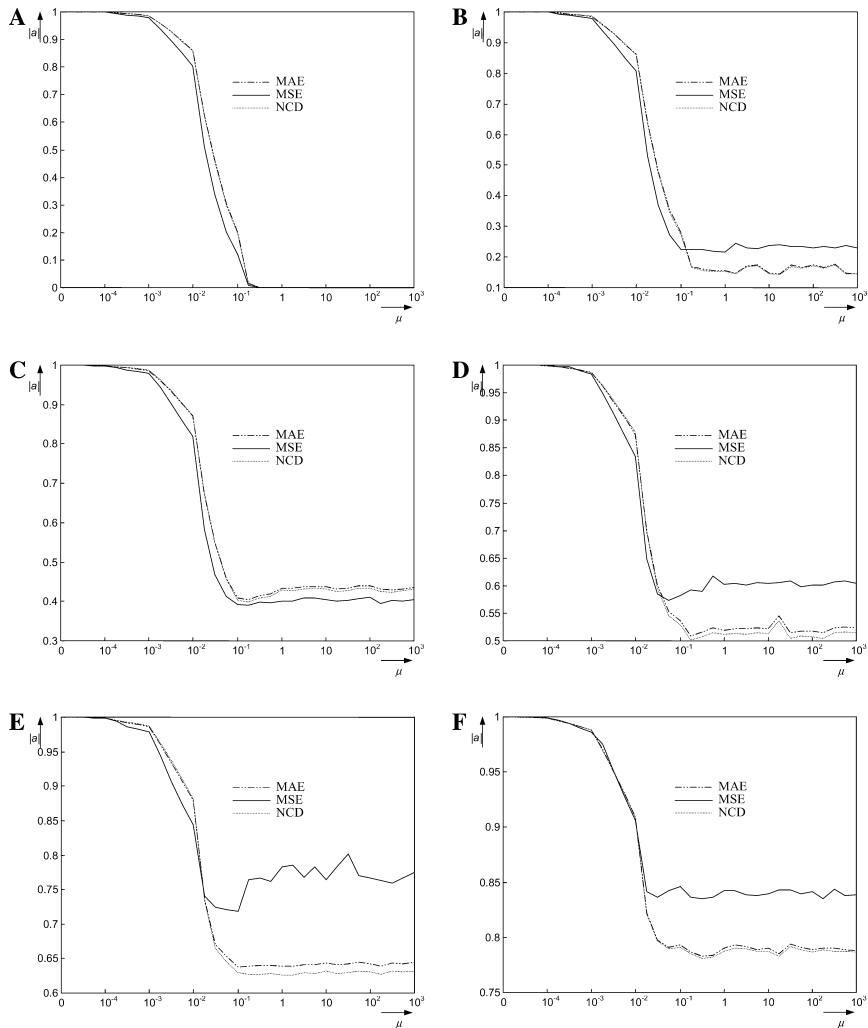


Fig. 5. WVDF sigmoidal optimization (SWVDF filter) expressed through normalized measures dependent on the iteration step size  $\mu$ . Training set was delivered by the image Lena with: (A) no corruption, (B) 2% impulsive noise, (C) 5% impulsive noise, (D) 10% impulsive noise, (E) 15% impulsive noise, and (F) 20% impulsive noise.

Fig. 4) was found to be around 0.001. For larger values of  $\mu$ , the LWVDF does not converge to sub-optimal solution and its performance is worse. In the case of the WVDF with sigmoidal approximation of the sign function (SWVDF), the most appropriate  $\mu$  was found (Fig. 5 and Fig. 6) to be around 0.1. For smaller  $\mu$  the SWVDF provides worse detail preserving characteristics and after some critical point, which depends on the statistical properties of the training sequence, it converges to the filtering operation close to the one performed by the BVDF.

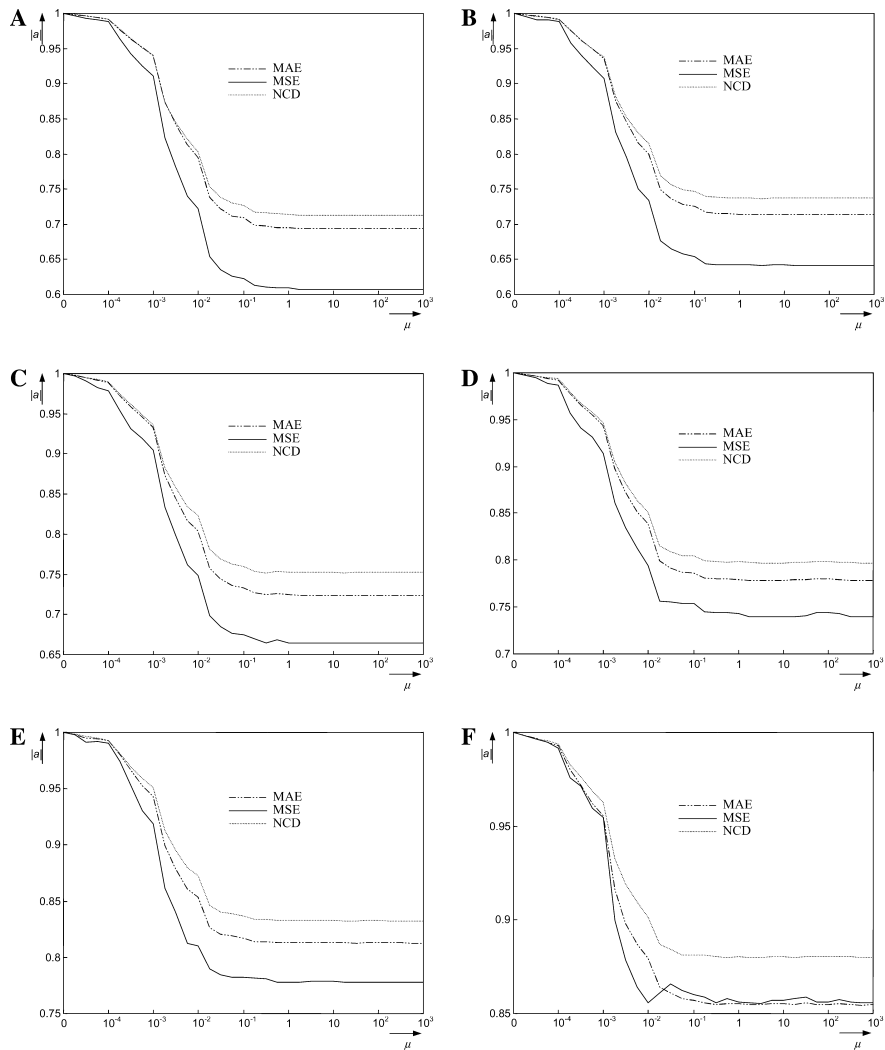


Fig. 6. WVDF sigmoidal optimization (SWVDF filter) expressed through quality measures dependent on the iteration stepsize  $\mu$ . Training set was given by the image Peppers: (A) no corruption, (B) 2% impulsive noise, (C) 5% impulsive noise, (D) 10% impulsive noise, (E) 15% impulsive noise, and (F) 20% impulsive noise.



Fig. 7. Achieved results related to image Lena degraded by 10% impulsive noise (training set). (A) VMF output, (B) BVDF output, (C) MF output, (D) WVDF1 output (E) LWVDF output, and (F) SWVDF output.

To achieve the robust weighting coefficients used throughout this paper, we used the test image LENA corrupted by 10% impulsive noise as the training set. The reason is that this image and the considered noise corruption represent a compromise between the image features complexity and the degree of noise corruption. After the optimization of the WVDF weight coefficients, we tested the performance of the new methods using both original and noisy images, performing a series of tests

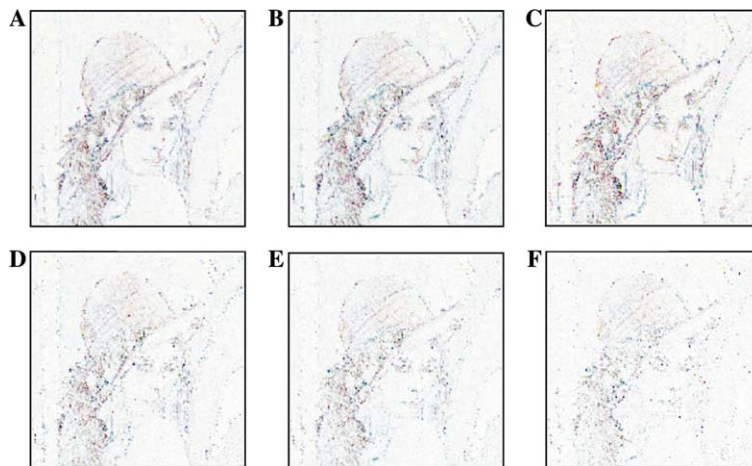


Fig. 8. Estimation errors emphasized by a factor of 2.5 related to the results shown in Fig. 7. (A) VMF, (B) BVDF, (C) MF, (D) WVDF<sub>1</sub>, (E) LWVDF, and (F) SWVDF.

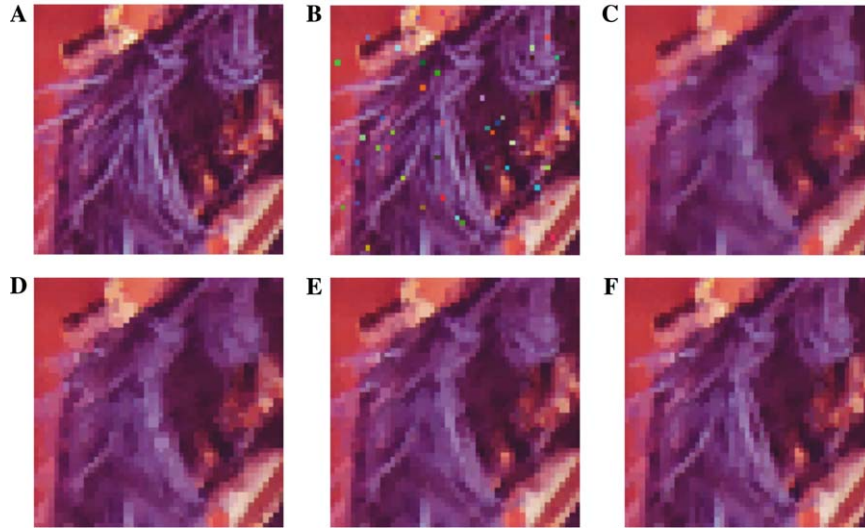


Fig. 9. Zoomed results obtained using the Lena test image. (A) original image, (B) noisy image (2% impulsive noise), (C) VMF output, (D) BVDF output, (E) LWVDF output, and (F) SWVDF output.

in which the images were corrupted by impulsive noise with a wide degree of noise corruption intensities. The considered image disturbance ranged from 0 to 20% impulsive noise with fixed stepsize 1%. These values correspond to the impulse probability  $p_v$  ranging from 0 to 0.20 with the fixed stepsize of 0.01.

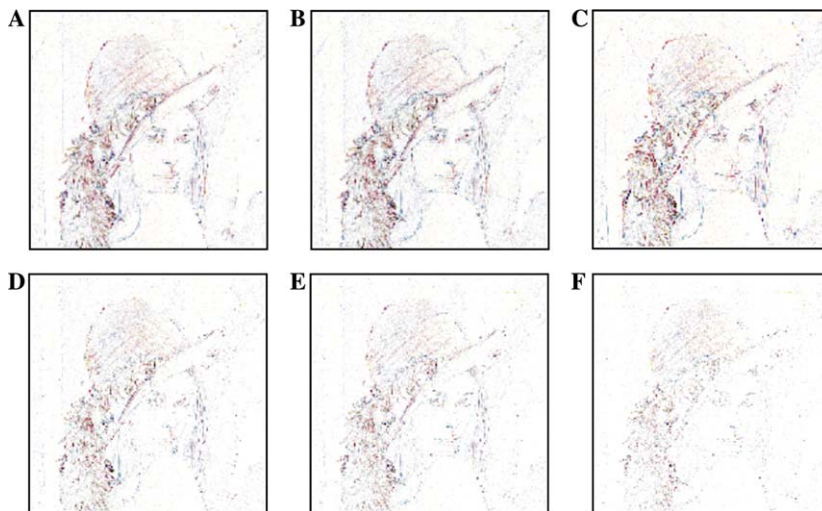


Fig. 10. Estimation errors emphasized by a factor of 2.5 related to the test image Lena degraded by 2% impulsive noise: (A) VMF, (B) BVDF, (C) MF, (D) WVDF<sub>1</sub>, (E) LWVDF, and (F) SWVDF.

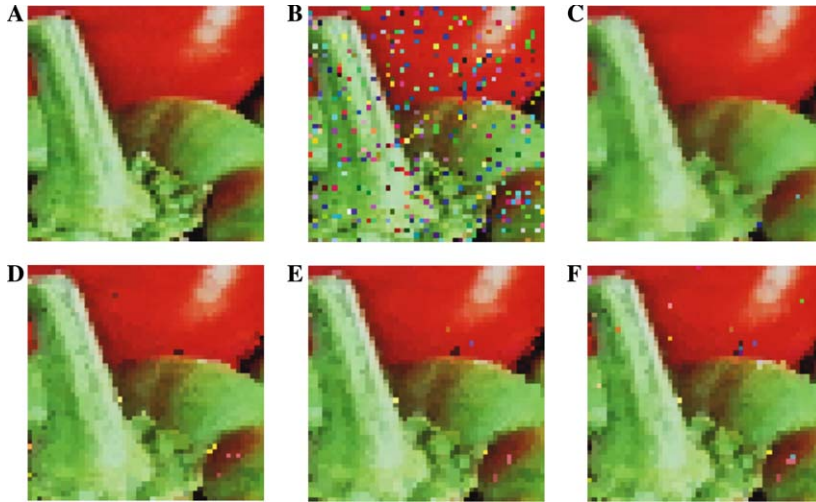


Fig. 11. Zoomed results related to test image Peppers. (A) original image, (B) noisy image (15% impulsive noise), (C) VMF output, (D) BVDF output, (E) LWVDF output, and (F) SWVDF output.

Fig. 7 shows the results related to the filtering of the training set. It can be observed that the optimal filters LWVDF (Fig. 7E) and SWVDF (Fig. 7F) provide improved signal-detail preservation capabilities in comparison with the componentwise MF (Fig. 7C) and standard vector filters such as VMF (Fig. 7A), BVDF (Fig. 7B). This behavior is more visible in Fig. 8, which corresponds to the estimation errors of

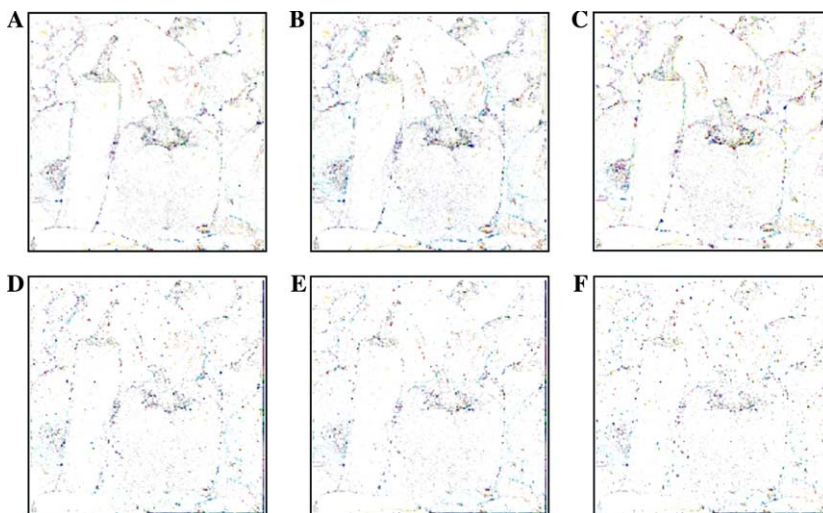


Fig. 12. Estimation errors emphasized by a factor of 2.5 related to the test image Peppers degraded by 15% impulsive noise: (A) VMF, (B) BVDF, (C) MF, (D) WVDF<sub>1</sub>, (E) LWVDF, and (F) SWVDF.

the above mentioned methods. Note, that the  $WVDF_1$  and the  $WVDF_2$  describe the non-optimized  $WVDFs$  with the weighting vectors  $[2,1,2,1,3,1,2,1,2]$  and  $[1,2,1,4,5,4,1,2,1]$ , respectively. The undesired effect of blurring of fine image details introduced by VMF, BVDF, and componentwise MF is shown in Figs. 8A–C. It can be easily observed that the VMF filter (Fig. 8A) excellently suppresses impulses present in the image, however some edges and image details are heavily blurred, especially at transitions between image regions. In the case of the BVDF, the

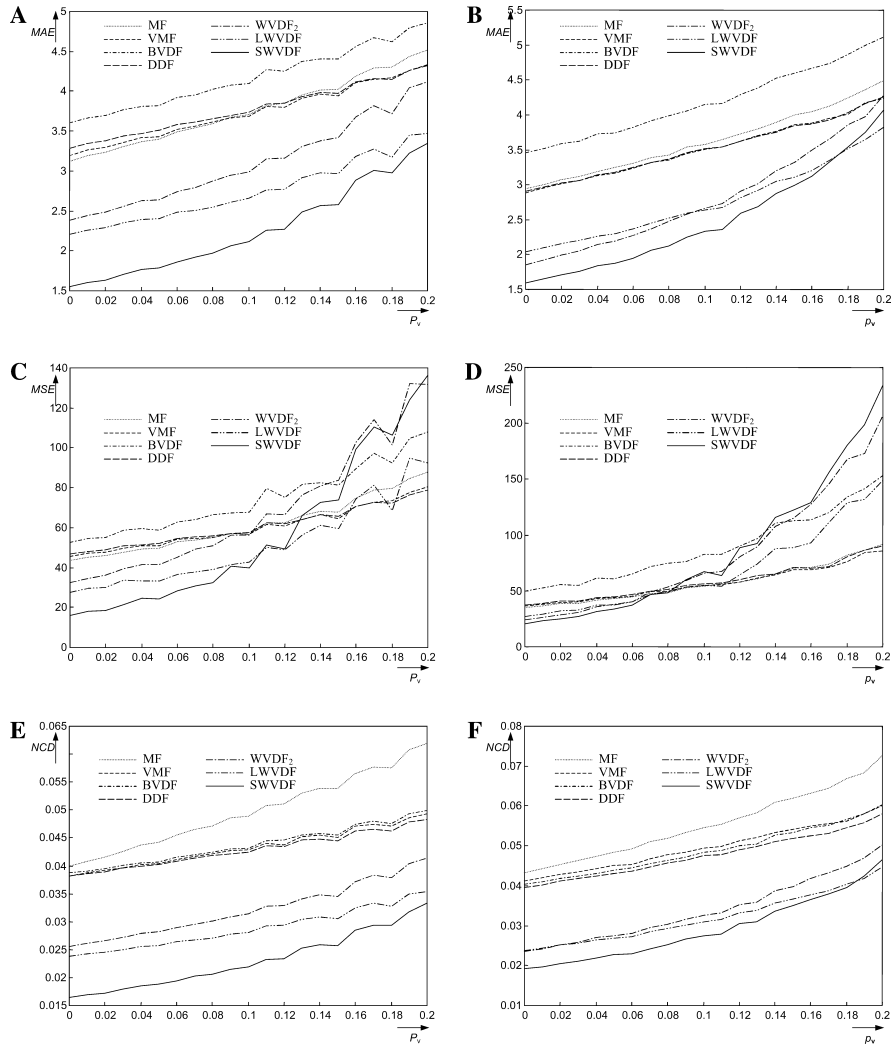


Fig. 13. Performance of the relevant methods for increasing intensity of the impulsive noise corruption. (A,C,E) test image Lena, (B,D,F) test image Peppers (A,B) MAE criteria, (C,D) MSE criteria, and (E,F) NCD criteria.

increased estimation error (Fig. 8B) is caused by pure directional processing. In some situations, the decreased noise attenuation capability of the BVDF can result in the presence of impulses in the filtered image. Since the DDF combines the properties of both VMF and BVDF, it can achieve better results than that of the BVDF and VMF. However, in the case of the MF, the corresponding image is often characterized (Fig. 8C) by larger estimation error than the VMF or BVDF, since its output usually represents a new image sample of different color in comparison with the desired neighborhood. The outputs (Figs. 7E and F) of the proposed LWVDF and SWVDF filters are characterized by an excellent balance between signal-detail preservation and the noise suppression. This results in very small estimation error depicted in Figs. 8E and F.

Figs. 9–12 show the results of the new methods when applied to images different from the training sequence. It can be observed again that the proposed LWVDF and SWVDF achieve better results than standard filters, despite the fact that the optimal WVDFs were optimized using the training set with different amount of injected noise.

The robust behavior of the new filters in environments corrupted by impulsive noise is presented in Fig. 13. These results correspond to the objective criteria dependent on degree of the noise corruption. Note that the intensity (probability) of impulsive noise ranged from  $p_v = 0$  to  $p_v = 0.20$  with the stepsize 0.01. In general, the proposed SWVDF framework provides the best signal-detail preservation expressed through the MAE measure. In the case of the NCD criteria, both optimal filters designed within the proposed WVDF framework provide the best results among the tested filters.

Tables 1–4 allow for the numerical, objective comparison of the results. Componentwise MF filter [46], standard vector filters (VMF [1], BVDF [39], and DDF [18]),

Table 1  
Comparison of the presented algorithms using original images

Image Method/ Criterion	Lena			Peppers		
	MAE	MSE	NCD	MAE	MSE	NCD
MF	3.123	43.5	0.03987	2.946	35.5	0.04330
VMF	3.190	45.4	0.03816	2.885	36.7	0.04111
BVDF	3.605	52.7	0.03870	3.458	50.2	0.04031
DDF	3.288	46.8	0.03812	2.907	37.5	0.03965
AVDF	4.112	50.2	0.04698	3.853	44.8	0.05248
GVDF	3.489	52.4	0.04124	3.350	50.4	0.04642
HVF <sub>1</sub>	3.341	46.1	0.03900	2.997	35.9	0.04082
HVF <sub>2</sub>	3.332	45.4	0.03894	2.992	35.5	0.04079
WVDF <sub>1</sub>	2.842	41.3	0.03063	2.690	40.1	0.03105
WVDF <sub>2</sub>	2.379	32.5	0.02557	1.852	23.9	0.02347
LWVDF	2.212	27.6	0.02378	2.043	27.2	0.02373
SWVDF	1.552	16.2	0.01644	1.596	20.4	0.01915

Table 2

Comparison of the presented algorithms using impulsive noise corruption  $p_v = 0.05$ 

Image Method/ Criterion	Lena			Peppers		
	MAE	MSE	NCD	MAE	MSE	NCD
Noisy	3.762	427.3	0.04450	3.988	486.1	0.04414
MF	3.394	49.7	0.04420	3.248	43.1	0.04841
VMF	3.430	50.8	0.04031	3.169	43.9	0.04520
BVDF	3.818	58.6	0.04073	3.740	60.7	0.04378
DDF	3.509	52.3	0.04023	3.182	44.6	0.04309
AVDF	4.301	54.3	0.04834	4.068	51.4	0.05522
GVDF	3.697	59.2	0.04301	3.605	62.5	0.04855
HVF <sub>1</sub>	3.587	51.8	0.04101	3.282	42.9	0.04413
HVF <sub>2</sub>	3.573	50.4	0.04095	3.274	41.9	0.04413
WVDF <sub>1</sub>	3.054	47.7	0.03267	2.974	52.2	0.03449
WVDF <sub>2</sub>	2.643	41.5	0.02826	2.197	38.1	0.02751
LWVDF	2.399	33.4	0.02569	2.296	37.6	0.02677
SWVDF	1.783	24.2	0.01885	1.876	33.9	0.02274

Table 3

Comparison of the presented algorithms using impulsive noise corruption  $p_v = 0.10$ 

Image Method/ Criterion	Lena			Peppers		
	MAE	MSE	NCD	MAE	MSE	NCD
Noisy	7.312	832.0	0.08401	7.677	943.3	0.08696
MF	3.703	56.8	0.04893	3.579	53.9	0.05463
VMF	3.687	56.5	0.04285	3.503	55.0	0.04935
BVDF	4.099	67.6	0.04321	4.151	82.7	0.04844
DDF	3.733	57.3	0.04240	3.512	56.6	0.04749
AVDF	4.540	59.5	0.05029	4.370	61.6	0.05946
GVDF	3.925	66.8	0.04481	3.862	72.7	0.05091
HVF <sub>1</sub>	3.857	56.9	0.04344	3.626	53.6	0.04855
HVF <sub>2</sub>	3.840	55.5	0.04339	3.614	52.4	0.04853
WVDF <sub>1</sub>	3.347	58.2	0.03537	3.399	77.1	0.03932
WVDF <sub>2</sub>	2.989	56.3	0.03138	2.659	65.9	0.03249
LWVDF	2.661	42.5	0.02810	2.642	55.2	0.03103
SWVDF	2.114	39.8	0.02192	2.330	67.3	0.02745

adaptive vector directional filter (AVDF) [32] and two hybrid vector filters (HVF<sub>1</sub> and HVF<sub>2</sub>) [12] are compared in terms of performance with the proposed non-optimized (WVDF<sub>1</sub> and WVDF<sub>2</sub>) and optimized (LWVDF and SWVDF) filters. These results again confirm that the proposed WVDF framework can be designed to provide an excellent trade-off between noise attenuation and signal-detail preserving characteristics. Moreover, the proposed framework outperforms basic filtering schemes in terms of the commonly used objective measures as well as visual compar-

Table 4  
Comparison of the presented algorithms using impulsive noise corruption  $p_v = 0.20$

Image Method/ Criterion	Lena			Peppers		
	MAE	MSE	NCD	MAE	MSE	NCD
Noisy	14.019	1604.6	0.16252	14.912	1832.0	0.16938
MF	4.521	87.9	0.06198	4.487	91.4	0.07266
VMF	4.335	80.3	0.04924	4.232	85.7	0.06008
BVDF	4.859	107.8	0.04987	5.111	152.9	0.06024
DDF	4.321	78.8	0.04834	4.254	90.4	0.05796
AVDF	5.258	80.4	0.05722	5.226	98.3	0.07394
GVDF	4.345	83.4	0.04928	4.395	106.5	0.05771
HVF <sub>1</sub>	4.548	80.4	0.05003	4.411	86.4	0.05998
HVF <sub>2</sub>	4.547	79.5	0.04999	4.409	84.5	0.05996
WVDF <sub>1</sub>	4.212	106.8	0.04306	4.571	167.2	0.05317
WVDF <sub>2</sub>	4.113	131.6	0.04141	4.275	206.5	0.05033
LWVDF	3.466	92.3	0.03533	3.824	148.6	0.04467
SWVDF	3.345	136.1	0.03333	4.064	234.1	0.04648

isons and significantly improves performance of directional processing based multi-channel filters.

## 7. Conclusion

An important task in nonlinear image filtering relates to developing of a unified theory, which would generalize a variety of existing nonlinear filters and provide versatile optimization algorithms. In this sense, we introduced a generalized WVDF framework for color image filtering based on the color vectors' directionality. New angular multichannel optimization algorithms of the WVDF weighting coefficients have been provided as well. The successful adaptation of the WVDFs to varying image noise statistics was confirmed by the presented results. The proposed filtering technique clearly outperforms the standard vector filters including widely used VMF and BVDF schemes. Moreover, the developed multichannel angular optimization is fast, saves memory space and is easy to implement. After the optimization, the proposed WVDFs are sufficiently robust and useful for practical image processing applications.

Future research will focus on the automatic setting of the adaptation parameter in the proposed filter class and the design of versatile self-adaptive optimization eliminating the need for a learning signal.

## Acknowledgments

The work of the first author is supported by a NATO/NSERC Science award. The work of the second author is supported by the KBN Grant 4T11F01824.

## References

- [1] J. Astola, P. Haavisto, Y. Neuvo, Vector median filters, *Proc. IEEE*. 78 (1990) 678–689.
- [2] J. Astola, P. Kuosmanen, *Fundamentals of Nonlinear Digital Filtering*, CRC Press, Boca Raton, 1997.
- [3] J. Astola, D. Akopian, A time-recursive implementation of threshold Boolean filters, *IEEE Trans. Circ. Syst.—II* 46 (1999) 139–148.
- [4] A.J. Bardos, S.J. Sangwine, Selective vector median filtering of colour images, in: *Proc. 6th International Conference on Image Processing and Its Applications*, 2, 1997, pp. 708–711.
- [5] M. Barni, F. Bartolini, V. Capellini, Image processing for virtual restoration of artworks, *IEEE Multimedia* (2000) 34–37.
- [6] C. Bonchelet, Image noise models, in: A. Bovik (Ed.), *Handbook of Image and Video Processing*, Academic Press, 2000.
- [7] E.J. Coyle, J.H. Lin, M. Gabbouj, Optimal stack filtering and the estimation and structural approaches to image processing, *IEEE Trans. Acoust., Speech, Signal Process.* 37 (1989) 2037–2066.
- [8] J. Dopazo, Microarray data processing and analysis, in: S.M. Lin, K.F. Johnson (Eds.), *Microarray Data Analysis II*, Kluwer Academic, 2002, pp. 43–63.
- [9] R.O. Duda, P.E. Hart, *Pattern Classification and Scene Analysis*, Wiley, New York, 1973.
- [10] M.B. Eisen, P.O. Brown, DNA arrays for analysis of gene expression, *Methods Enzymol.* 303 (1999) 179–205.
- [11] M. Fischer, J.L. Paredes, G.R. Arce, Weighted median image sharpeners for the world wide web, *IEEE Trans. Image Process.* 11 (2002) 717–727.
- [12] M. Gabbouj, A. Cheickh, Vector median-vector directional hybrid filter for color image restoration, in: *Proc. EUSIPCO-1996*, 1996, pp. 879–881.
- [13] N.J. Garber, L.A. Hoel, *Traffic and Highway Engineering*, Brooks/Cole Publishing, Pacific Grove, CA, 1999.
- [14] Y. Hashimoto, Y. Kajikawa, Y. Nomura, Directional difference-based switching median filters, *Electron. Commun. Jpn.* 85 (Part 3) (2002) 22–32.
- [15] Y. Hashimoto, Y. Kajikawa, Y. Nomura, Directional difference filters: its effectiveness in the postprocessing of noise detectors, *Electron. Commun. Jpn.* 85 (Part 3) (2002) 74–82.
- [16] S. Kalluri, G.R. Arce, Adaptive weighted myriad filter algorithms for robust signal processing in a-stable noise environments, *IEEE Trans. Signal Process.* 46 (1998) 322–334.
- [17] S. Kalluri, G.R. Arce, Robust frequency-selective filtering using weighted myriad filters admitting real-valued weights, *IEEE Trans. Signal Process.* 49 (2001) 2721–2733.
- [18] D.G. Karakos, P.E. Trahanias, Generalized multichannel image-filtering structure, *IEEE Trans. Image Process.* 6 (1997) 1038–1045.
- [19] A. Kokaram, *Motion Picture Restoration*, Springer-Verlag, Berlin, 1998.
- [20] X. Li, D. Lu, Y. Pan, Color restoration and image retrieval for donhunag fresco preservation, *IEEE Multimedia* (2000) 38–42.
- [21] L. Lucat, P. Siohan, D. Barba, Adaptive and global optimization methods for weighted vector median filters, *Signal Process. Image Commun.* 17 (2002) 509–524.
- [22] R. Lukac, Color image filtering by vector directional order-statistics, *Pattern Recognit. Image Anal.* 12 (2002) 279–285.
- [23] R. Lukac, Binary LUM smoothing, *IEEE Signal Process. Lett.* 9 (2002) 400–403.
- [24] R. Lukac, Adaptive vector median filtering, *Pattern Recognit. Lett.* 24 (2003) 1889–1899.
- [25] R. Lukac, B. Smolka, K.N. Plataniotis, A.N. Venetsanopoulos, Vector Filtering for Color Imaging, *IEEE Signal Processing Magazine*, Special Issue on Color Image Processing, to appear.
- [26] S. Mitra, J. Sicuranza, *Nonlinear Image Processing*, Academic Press, 2001.
- [27] N. Nikolaidis, I. Pitas, directional statistics in nonlinear vector field filtering, *Signal Process.* (1994) 299–316.
- [28] S. Peltonen, M. Gabbouj, J. Astola, Nonlinear filter design: methodologies and challenges, in: *Proc. ISPA'01*, 2001, pp. 102–106.

- [29] I. Pitas, A.N. Venetsanopoulos, *Nonlinear Digital Filters, Principles and Applications*, Kluwer Academic Publishers, 1990.
- [30] I. Pitas, P. Tsakalides, Multivariate ordering in color image filtering, *IEEE Trans. Circ. Syst. Video Technol.* 1 (1991) 247–259.
- [31] I. Pitas, A.N. Venetsanopoulos, Order statistics in digital image processing, *Proc. IEEE*. 80 (1992) 1892–1919.
- [32] K.N. Plataniotis, D. Androutsos, A.N. Venetsanopoulos, Adaptive fuzzy systems for multichannel signal processing, *IEEE Proc. IEEE* 87 (1999) 1601–1622.
- [33] K.N. Plataniotis, A.N. Venetsanopoulos, *Color Image Processing and Applications*, Springer Verlag, Berlin, 2000.
- [34] H. Rantanen, M. Karlsson, P. Pohjala, S. Kalli, Color video signal processing with median filters, *IEEE Trans. Consumer Electron.* 38 (1992) 157–161.
- [35] G. Sharma, H.J. Trussel, Figures of merit for color scanners, *IEEE Trans. Image Process.* 6 (1997) 990–1001.
- [36] B. Smolka, K.N. Plataniotis, A. Chydzinski, M. Szczepanski, A.N. Venetsanopoulos, K. Wojciechowski, Self-adaptive algorithm of impulsive noise reduction in color images, *Pattern Recognit.* 35 (2002) 1771–1784.
- [37] M. Szczepanski, B. Smolka, K.N. Plataniotis, A.N. Venetsanopoulos, On the geodesic paths approach to color image filtering, *Signal Process.* 83 (2003) 1309–1342.
- [38] K. Tang, J. Astola, Y. Neuvo, Nonlinear multivariate image filtering techniques, *IEEE Trans. Image Process.* 4 (1995) 788–798.
- [39] P.E. Trahanias, D. Karakos, A.N. Venetsanopoulos, Directional processing of color images: theory and experimental results, *IEEE Trans. Image Process.* 5 (1996) 868–881.
- [40] T. Viero, K. Oistamo, Y. Neuvo, Three-dimensional median related filters for color image sequence filtering, *IEEE Trans. Circ. Syst. Video Technol.* 4 (1994) 129–142.
- [41] M. Wild, Idempotent and co-idempotent stack filters and min-max operators, *Theor. Comput. Sci.* (2003) 603–631.
- [42] R. Yang, L. Yin, M. Gabbouj, J. Astola, Y. Neuvo, Optimal weighted median filtering under structural constraints, *IEEE Trans. Signal Process.* 43 (1995) 591–604.
- [43] L. Yin, J. Astola, Y. Neuvo, Adaptive stack filtering with application to image processing, *IEEE Trans. Signal Process.-II* 41 (1993) 162–184.
- [44] L. Yin, Y. Neuvo, Fast adaptation and performance characteristics of FIR-WOS hybrid filters, *IEEE Trans. Signal Process.-II* 41 (1994) 1610–1628.
- [45] P.T. Yu, W.H. Liao, Weighted order statistics filters—their classification, some properties, and conversion algorithm, *IEEE Trans. Signal Process.* 42 (1994) 2678–2691.
- [46] J. Zheng, K.P. Valavanis, J.M. Gauch, Noise removal from color images, *J. Intel. Robot. Syst.* 7 (1993) 257–285.